Digital holographic recording and reconstruction of large scale objects for metrology and display

Jan Mundt
Thomas Kreis, MEMBER SPIE
Bremer Institut für angewandte Strahltechnik - BIAS
Klagenfurter Strasse 2
28359 Bremen, Germany
E-mail: kreis@bias.de

Abstract. Digital holography captures holograms by charge-coupled device or complementary metal-oxide semiconductor cameras, which have a spatial resolution still not reaching that of silver-halide holofilms. Thus, due to the sampling theorem, the angle between the reference and object wave is limited. Only fields coming from small objects, objects far away, or optically reduced fields can be recorded. Here we investigate optical reduction by a system of lenses, and show that a system of two concave lenses results in a drastic reduction of the object-target distance, while the effect of using more lenses is insignificant. Experimental results obtained with Fresnel and lensless Fourier-transform geometry are presented, and implications on holographic interferometric metrology as well as on holographic 3-D television are given. [DOI: 10.1117/1.3524238]

Subject terms: digital holography; numerical hologram reconstruction; holographic arrangements; optical metrology; holographic nondestructive testing; holographic 3-D television.

Paper 100641R received Aug. 5, 2010; revised manuscript received Oct. 26, 2010; accepted for publication Oct. 26, 2010; published online Dec. 17, 2010.

1 Introduction

Holography is a method for the capture and reconstruction of 3-D optical wave fields, which has found numerous applications in metrology and display technology. It is used in particle and flow detection,[1–3] and holographic interferometry is applied for form and deformation measurement,[4,5] as well as refractive index measurement.[6,7] It is a precise and well established method for experimental stress analysis as well as holographic nondestructive testing.[8–10] On the other hand, it is the most promising approach to 3-D TV, being the only 3-D reconstruction method that displays the real 3-D field, and not only giving the parallax effect, as stereoscopy does.[11,12] Holographic recording onto high-resolution holographic plates and films has been almost totally replaced today by digital holography, meaning recording of the hologram by the target of a digital charge-coupled device (CCD) or complementary metal-oxide semiconductor (CMOS) camera without focusing optics, followed by numerical instead of optical reconstruction.

Digital holography offers many advantages over classical holography, as there is the avoidance of wet chemical processing, no need for exact replacement of hologram plates, unlimited reusability of targets, and direct numerical access to amplitude and phase. The main drawback of digital holography is the up-to-now limited resolution of the CCD/CMOS targets compared to high-resolution holographic emulsions on plates or sheets. Due to the sampling theorem, the angle between object and reference wave remains limited, where the maximum allowable angle depends on the pixel pitch of the used target. However, it has been shown that the angular spectrum can be reduced optically by employing a concave lens,[13] so that even the wave fields reflected from large scale objects can be recorded by digital holography.

This concept is further elaborated in this work by using systems of more than one lens. We show how the holographic arrangement is optimized with regard to the distance between object surface and recording target. We also discuss what is economically feasible and where the method is still limited.

2 Digital Holography

Let the array used for digital recording of the microinterference pattern establishing the hologram have $N \times M$ light sensitive pixels with pixel pitch $\Delta\xi$ and $\Delta\eta$, which are the distances between pixel centers in ξ and η directions. In most cases we have $N = M$ and $\Delta\xi = \Delta\eta$, which is assumed in the following. Figure 1 shows schematically an arrangement for recording a digital Fresnel hologram with a normally impinging plane reference wave. Let θ be the angle between the reference wave and the wave emitted from object point P and hitting any hologram point H. Then the period p of the interference pattern caused by this point at H is

$$p = \frac{\lambda}{2\sin(\theta/2)}. \tag{1}$$

If the sampling theorem is fulfilled, then it is generally guaranteed that the hologram can be perfectly reconstructed from its samples, meaning no significant information is lost by sampling. However, in special cases with additional effort, it is possible to recover the signal even for angle values beyond the Nyquist limits.[14] The sampling theorem requires sampling of the period p with more than two pixels, thus

$$p > 2\Delta\xi. \tag{2}$$

Since θ remains small, we can set $\sin(\theta/2) = \theta/2$, and from Eqs. (1) and (2) we obtain

$$\theta < \frac{\lambda}{2\Delta\xi}. \tag{3}$$

As an example, this means for a pixel pitch $\Delta\xi = 3.45$ μm and $\lambda = 0.532$ μm, θ has to remain less than 4.4 deg.

The maximum allowed angle θ gives us the minimum distance d, where the object, here assumed as a plane object,

0091-3286/2010/$25.00 © 2010 SPIE

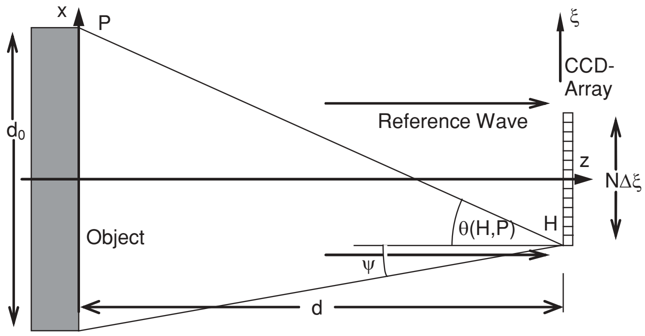

Fig. 1 Geometry for recording a digital Fresnel hologram.

can be placed. Assuming Fresnel geometry with the normally impinging plane reference wave of Fig. 1, we have

$$\tan\theta = \frac{\frac{d_O}{2} + \frac{N\Delta\xi}{2}}{d}, \tag{4}$$

where d_O is the maximum lateral object width. This θ is calculated for the symmetric arrangement of object and target, which gives the smallest θ for all arrangements as long as $N\Delta\xi < d_O$. With Eq. (3) and assuming a small θ, we obtain

$$\frac{\frac{d_O}{2} + \frac{N\Delta\xi}{2}}{d} < \frac{\lambda}{2\Delta\xi}, \tag{5}$$

which can be solved for d by

$$d > \frac{(d_O + N\Delta\xi)\Delta\xi}{\lambda}. \tag{6}$$

As a rule of thumb, the distance between object and target must obey $d > d_O\Delta\xi/\lambda$, which corresponds to the requirement that each object surface point fulfills the sampling theorem for at least half of the target points. Since these limits are exactly valid only for the marginal points of the object, the resulting loss in accuracy in the reconstructed wave file in this case is neglectable.

A further problem in digital holography is the occurance of the zero diffraction order, also known as the dc term. Using Fresnel holography with a plane reference wave as shown before, the dc term has a lateral extension of $[N^2\Delta\xi^2/(d\lambda)] \cdot \Delta\xi$ of the total $N \cdot \Delta\xi$ in each dimension of the reconstructed wave field. This poses no problem as long as we reconstruct the wave fields numerically, because there are algorithms suppressing the dc term during reconstruction.[15] But if one intends to reconstruct the wave fields optically by feeding the digital holograms to a spatial light modulator as in holographic TV, then the dc term plays a crucial role. Therefore, one has to place the object in a way not to overlap with the dc term. An elegant solution to this problem is to use the geometry of lensless Fourier-transform holography. Here a divergent reference wave with a source point in the plane of the object surface is employed, leading to a much smaller dc term in the reconstructed image, which in many cases even collapses to a single pixel.[16]

Since the hologram is an intensity distribution described only by real numbers, the reconstructed wave fields besides the dc term consist of a direct and conjugate image, the so-called twin images. While in Fresnel holography one of them is sharp and the other is unsharp, in lensless Fourier-transform holography both are sharp. No twin images occur if we record the complex field in the hologram plane, which can be performed by the phase shift methods. In temporal phase shifting methods, several real holograms are recorded consecutively with mutual constant phase shifts added.[17] The complex field then is calculated by solving a system of equations for each pixel. In spatial phase shift procedures, a linearly increasing spatial phase shift is added in a single hologram, and reconstruction of the wave field in the hologram plane is performed by Fourier-transform evaluation.[18,19] Since phase shifting needs much more effort and is more complicated, it is more costly and thus often avoided. Fresnel holography conceptually requires the most easy arrangement but produces a rather large dc term and an unsharp twin image, which can spread partially over the desired reconstructed image. Therefore, for holographic 3-D television, lensless Fourier-transform holography is recommended, while for metrologic problems, both methods are applicable due to the possibility of numerical elimination of twin image and dc term in digital Fresnel holography. Nevertheless, for any of these methods, the sampling theorem has to be fulfilled, which can be done by restricting to objects with small dimensions, or by placing the object far from the recording array. But there is the third possibility of reducing the angle θ, which can be performed by one or more lenses. This is shown in the following sections.

3 Arrangement with Single Lens

The angle θ between the line connecting a point of the object surface with a target point, and the direction of the reference wave in this target point fixes the spatial frequency of the hologram microinterference pattern in the target point. This spatial frequency can be reduced by introduction of a lens, as depicted in Fig. 2, for the case of a concave lens and a normally impinging plane reference wave. As seen from the CCD, the wave field seems to come from the small virtual image of the object, but not any more directly from the object. Let the lateral extension of the object be d_O, then the corresponding extension of the virtual image is d_V. So we have a transversal magnification $M_T = d_V/d_O = -f/(g - f)$, which in fact is a reduction. Here f is the (negative) focal length of the concave lens, and g is the distance of the object's surface from the lens. The lens formula $1/f = 1/g - 1/b$ gives the distance b of the virtual image from the lens. Now given the desired angle θ, the focal length of the lens f, the distance g between lens and object, and the object's extension d_O, we can calculate the distance a of the lens from the CCD. Having $\tan\theta = d_V/[2(a + b)]$,

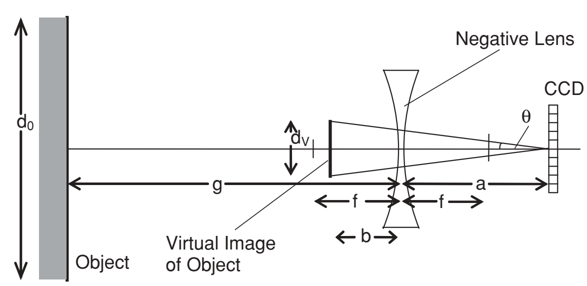

Fig. 2 Reduction of angular spectrum by single concave lens.

$d_V = -d_O f/(g - f)$, and $b = gf/(f - g)$, we obtain

$$a = \frac{-d_O\ f}{2(g - f)\tan\theta} - \frac{gf}{f - g}, \tag{7}$$

or if λ and $\Delta\xi$ are given, with Eq. (3) it follows

$$a > \frac{-d_O\ f\ \Delta\xi}{(g - f)\lambda} - \frac{gf}{f - g}. \tag{8}$$

Equation (8) gives the lens-CCD distance $a = a(g)$ as a function of g, the object-lens distance. So the total object-CCD distance d is $d = a + g$. The minimum distance between object and CCD now is obtained by minimizing $a(g) + g$. As an example, let $d_O = 500$ mm, $\Delta\xi = 3.45\ \mu$m, $\lambda = 0.532\ \mu$m, and $N = 2452$, then without a lens, a distance between object and CCD of more than 3.2 m is required. With a concave lens of $f = -50$ mm, this length can be reduced to a little bit more than $a + g = 0.7$ m.

If we use a convex lens instead of the concave one, Eq. (7) is replaced by

$$a = \frac{+d_O\ f}{2(g - f)\tan\theta} - \frac{gf}{f - g}. \tag{9}$$

Due to the now positive sign of the focal length, generally the total length of the holographic setup $a + g$ is larger than in the case of a concave lens.

4 Arrangement with Two Lenses

A typical arrangement employing two concave lenses with focal lengths f_1 and f_2, respectively, is shown in Fig. 3. The collimated reference wave here appears a little bit inclined, which is due to the off-axis geometry and results in a nonoverlapping of the reconstructed image with the dc term. g_1 and g_2 are the object distances, while b_1 and b_2 are the image distances related to lenses 1 and 2, respectively. Its operation can be described by lens 1 producing a first virtual image of size d_{V1} of the original object having size d_O, while lens 2 produces a further virtual image of size d_{V2}, now with the first virtual image acting as its original. Let us call them image 1 and image 2. If lens 1 has a distance from the object surface of g_1, then image 1 is the distance b_1 in front of the lens with

$$b_1 = \frac{f_1\ g_1}{g_1 - f_1}. \tag{10}$$

With the distance d_L between the two lenses, image 1 is $g_2 = b_1 + d_L$ apart from lens 2, so that the distance of virtual

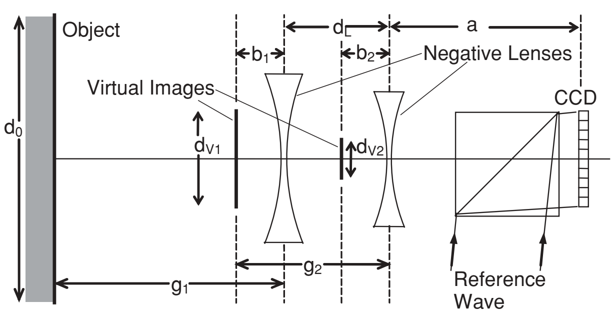

Fig. 3 System consisting of two concave lenses.

image 2 from lens 2 is calculated by

$$b_2 = \frac{f_2\ g_2}{g_2 - f_2} = \frac{d_L f_2 + f_1 f_2 g_1/(g_1 - f_1)}{d_L - f_2 + f_1 g_1/(g_1 - f_1)} = \frac{d_L f_2(g_1 - f_1) + f_1 f_2 g_1}{(d_L - f_2)(g_1 - f_1) + f_1 g_1}. \tag{11}$$

The resulting magnification M_T is

$$M_T = M_{T1} M_{T2} = \frac{d_{V2}}{d_O} = \frac{b_1}{g_1}\frac{b_2}{g_2} = \frac{f_1 f_2/(g_1 - f_1)}{d_L - f_2 + f_1 g_1/(g_1 - f_1)} = \frac{f_1 f_2}{(d_L - f_2)(g_1 - f_1) + f_1 g_1}. \tag{12}$$

The distance $a + b_2$ from image 2 to the CCD now depends on the limiting angle θ, and a is given by

$$a = \frac{d_O f_1 f_2}{2\tan\theta[(d - f_2)(g_1 - f_1) + f_1 g_1]} - b_2, \tag{13}$$

so that the total length of the arrangement is $d = a + g_1 + d_L$, which can be made less than the total length $a + g$ using one lens, as is demonstrated in the next section.

5 Optimal Number of Lenses

In the same way as described in the preceding sections, the distance between object surface and CCD can be calculated for three, four, or even more lenses. However, the formulas become increasingly clumsy. But this procedure allows us to compute and compare the achievable reduction of the length of the holographic arrangement. These simulations with up to four lenses have been performed for a typical set of parameters, which correspond to the experiments executed in this context. Without loss of generality, concave lenses of three different focal lengths have been used, but for better comparison of the results, only combinations of lenses with identical focal lengths were utilized. The focal lengths are −100, −50, and −25 mm. The pixel number is that of the Pike F-505B camera of Allied Vision Technology (Stadtroda, Germany), with $N = 2452$ pixels in the horizontal direction. The pixel pitch is $\Delta\xi = 3.45\ \mu$m, and the wavelength of the frequency-doubled Nd:YAG laser also used in the experiments is $\lambda = 0.532\ \mu$m. An object diameter of 180 mm is chosen. Recognizing the fact, that the a calculated in Eq. (13) is $a(g_1, d_L)$ for the two lenses, the object-CCD distance d is also a function of g_1 and d_L in this case, so the minimization is performed over varying g_1 and d_L. Furthermore, an off-axis arrangement has been chosen to avoid mutual overlapping of the reconstructed plus and minus first diffraction orders, as well as overlapping with the dc term.

The results of the calculations are depicted in Fig. 4. We recognize the same trend for all focal lengths: a drastic decrease of object-CCD distance by introduction of the first lens, and a reasonable further decrease by taking two lenses. However, the effects of a third or even fourth lens are not significant. Also, a larger number of lenses would complicate the setup and could introduce additional aberrations. So as a good compromise between the desire for a short arrangement and a low number of components, the utilization of two lenses is recommended. Furthermore, Fig. 4 indicates that nearly the same effects can be obtained by one or more

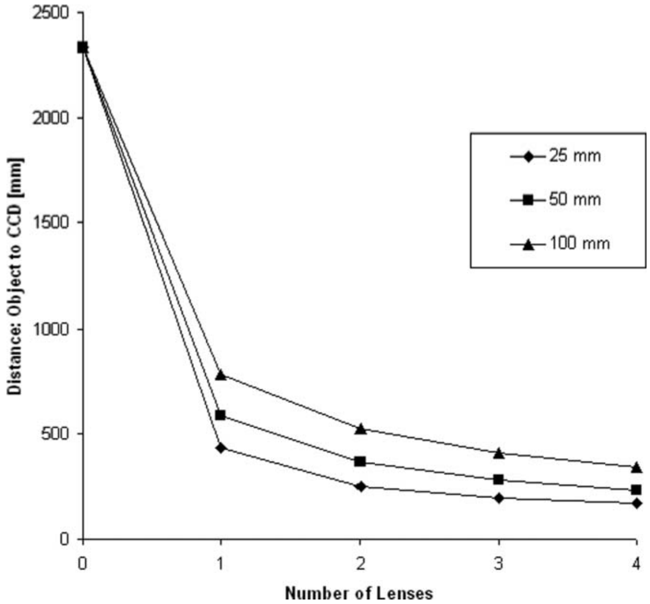

Fig. 4 Object-to-CCD distance versus number of lenses.

lenses with other focal lengths, e.g., the distance when using two lenses with focal lengths −100 mm is the same result as one lens with focal length −50 mm. Here the user can choose, with the objective of minimizing spherical and other aberrations due to the thicknesses of the lenses.

6 Experimental Results

The feasibility of the optical field reduction by two lenses has been tested experimentally using an object height of 18 cm, a statuette of the Bremen Town Musicians. This object was recorded using the Fresnel-type holographic arrangement, as shown in Fig. 5. By proper choice of the lenses L_{R1} and L_{R2} in the reference arm, Fresnel holography with a normally impinging plane reference wave as well as lensless Fourier transform holography can be used. The object is illuminated simultaneously from two directions to prevent shadowing. A photograph of the setup with two lenses having focal lengths $f_1 = -75$ mm and $f_2 = -50$ mm is presented in Fig. 6. The intensity field numerically reconstructed from a digital hologram recorded with Fresnel geometry is shown in Fig. 7. The statuette reconstructed in the positive first diffraction order is placed right of the rectangular dc term. The extremely unsharp negative first order has such low contrast that it is not recognizable in the display.

The experiment has been repeated by using the lensless Fourier-transform arrangement of Fig. 8. R is the virtual source point of the now divergent reference wave. This R is in the plane of the object, which is the small virtual object seen from the CCD due to the two lenses. The intensity distribution reconstructed from the hologram recorded with this setup is displayed in Fig. 9. Here the positive as well as the negative first order both are sharply reconstructed. The statuette recorded and reconstructed holographically has a height of 18 cm and a width of about 12 cm. Since both diffraction orders must fit into the pixel array, the width must fit two times into the field, together with a nonoverlapping dc term. This demonstrates the advantages of lensless Fourier-transform holography because of its small dc term.

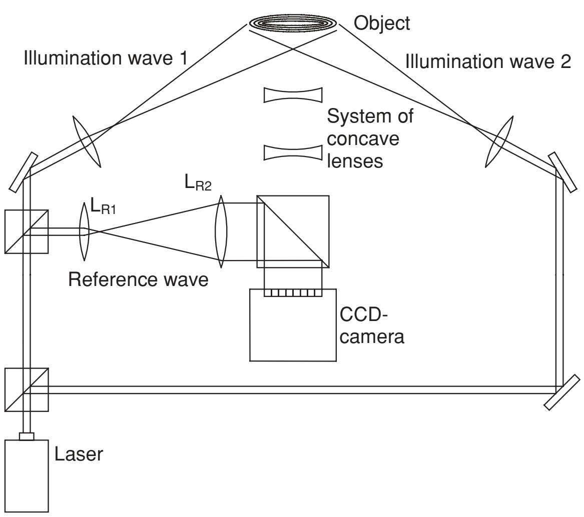

Fig. 5 Scheme of holographic arrangement.

Fig. 6 Two-lens arrangement.

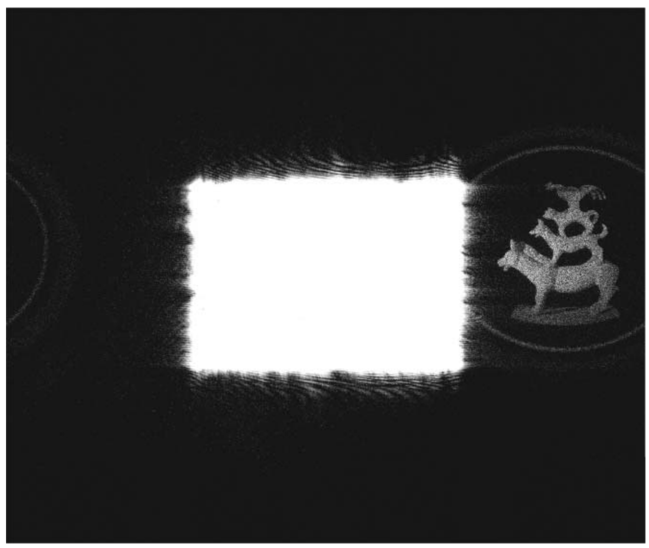

Fig. 7 Reconstructed intensity; hologram recorded with Fresnel geometry.

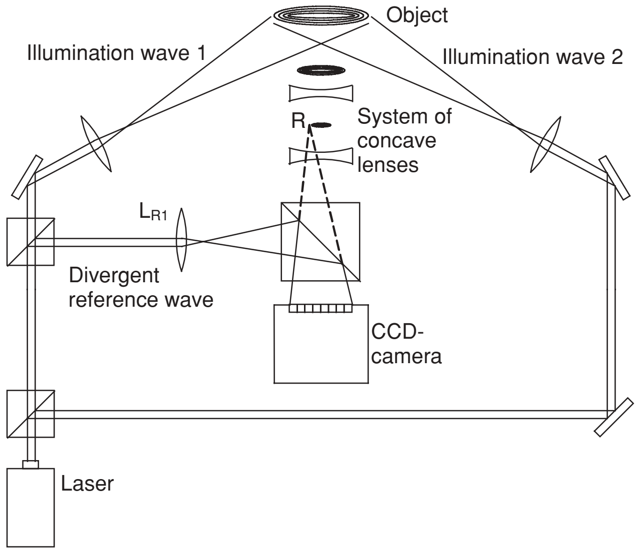

Fig. 8 Two-lens arrangement for lensless Fourier-transform holography.

The reconstructed wave field exhibits some geometrical distortions, which can be detected most clearly in the plane pedestal that is imaged slightly curved. But the most remarkable fact is that the distance between object and CCD is less than 22 cm, while without the lenses more than 1.5 m would be necessary.

7 Conclusions

We show theoretically and prove experimentally that the small object angle dictated by the sampling theorem can be obtained by using a single lens or a system of several lenses. By a lens system, the angle between object wave and reference wave in holography can be kept small, or in other words, the spatial frequency spectrum in the hologram can be reduced. If the principal criterion is a short distance between the object surface and recording CCD target, concave lenses are recommended. Simulations show that more than two lenses reduce the object-CCD distance only insignificantly compared to a two-lens system. Two-lens systems are therefore the best choice. For metrology applications, where we deal with the numerically reconstructed intensity and phase fields, Fresnel geometry is feasible, because the dc term can be elimininated numerically. If, on the other hand, the purpose is holographic 3-D television, when dealing with an intensity hologram the dc term cannot be eliminated, so the lensless Fourier-transform geometry is favored, since it has the smallest dc term. So by using lensless Fourier transform holography and an optical system, we reach an arrangement with less than 25-cm distance between object and CCD. If the CCD array has different pixel numbers in ξ and η directions, or if the extent of the object is different in x and y directions, then there is an optimal exploitation of the pixel array. Since both the first diffraction orders and the dc term are reconstructed simultaneously, the object should be placed in a way that in one direction the zero and both first orders fit into the pixel array, while the other direction can be fully occupied by the object height or width.

The experiments presented in this work exhibit clearly visible aberrations in the numerically reconstructed wave fields. In future research work, these aberrations are to be minimized by a combination of concave and convex lenses, or they will be compensated by an analog optical lens system in the optical reconstruction process in holographic 3-D TV. For numerical reconstruction, furthermore, there exist effective algorithms for computer-aided correction of these anamorphic images.[20,21] The proposed approach to reduce the object angle is not a direct solution to the keyhole problem of digital

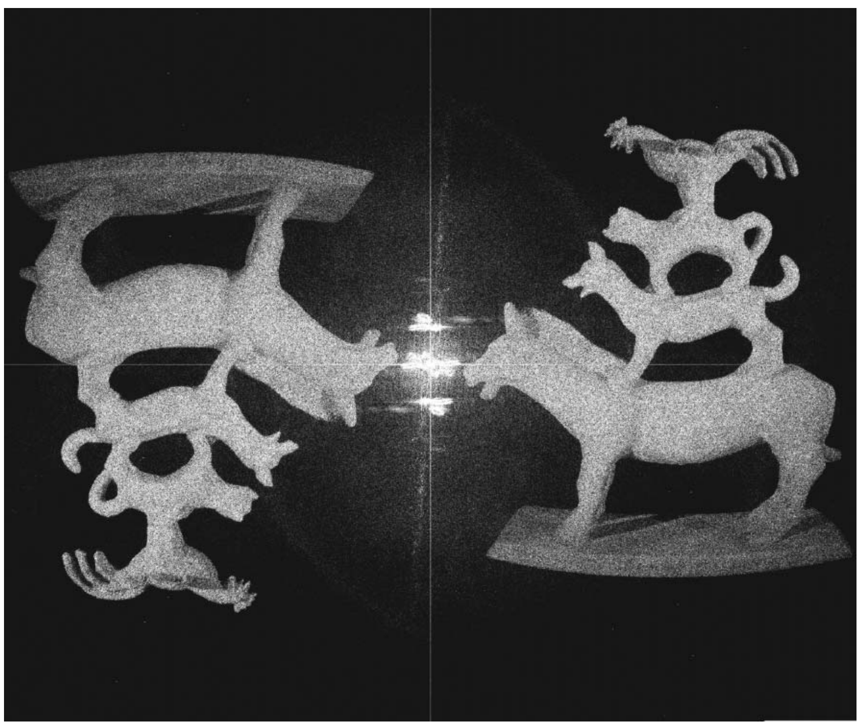

Fig. 9 Reconstructed intensity; hologram recorded with lensless Fourier-transform geometry.

holography, which means that the object is seen from only a short angle, like looking through a keyhole. But it paves the way to design optical systems with a large-diameter front lens near the object, thus allowing the object not only to be seen from one direction, but simultaneously from a continuum of angular directions, thus offering enhanced 3-D capability.

Acknowledgments

The authors thank Silke Huferath-von Lüpke and Thomas Meeser for valuable discussions, and Ralf Bergmann for his support of the project. The research was funded by the European Community's Seventh Framework Programme FP7/2007-2013, grant 216105 (project REAL3 D).

References

1. G. Pan and H. Meng, "Digital holography of particle fields: reconstruction by use of complex amplitude," *Appl. Opt.* **42**(5), 827–833 (2003).
2. J. D. Trolinger, "The new methods in holographic flow diagnostics," *SEM Intl. Conf. Hologram Interferometry Speckle Metrology*, pp. 488–493 (1990).
3. T. Kreis, M. Adams, and W. Jüptner, "Digital in-line holography in particle measurement," *Proc. SPIE* **3744**, 54–64 (1999).
4. N. Abramson, *The Making and Evaluation of Holograms, Academic Press*, San Diego, CA (1981).
5. T. Kreis, "Computer-aided evaluation of holographic interferograms," in *Holographic Interferometry*, P. K. Rastogi, Ed., Springer Series in Optical Sciences, Vol. 68, pp. 151–212 (1994).
6. S. S. Cha and H. Sun, "Tomography for reconstructing continuous fields from ill-posed multidirectional interferometric data," *Appl. Opt.* **29**(2), 251–258 (1990).
7. T. Kreis, "Digital holography for metrologic applications," in *Interferometry in Speckle Light*, P. Jacquot and J. M. Fournier, Eds., pp. 205–212, Springer-Verlag, Berlin (2000).
8. J. E. Sollid and K. A. Stetson, "Strains from holographic data," *Exp. Mech.* **18**(6), 208–214 (1978).
9. G. Birnbaum and C. M. Vest, "Holographic nondestructive evaluation: status and future," *Intern. Adv. Nondestruct. Test.* **9**, 257–282 (1983).
10. T. Kreis, *Handbook of Holographic Interferometry*, Wiley-VCH, New York (2005).
11. K. Iizuka, "Welcome to the wonderful world of 3D: introduction, principles and history," *OPN*, pp. 43–51 (2006).
12. T. Kreis, "Digital holography methods in 3D-TV," *IEEE Proc. 3DTV-Con 01 The True Vision-Capture, Transmission and Display of 3D Video* (2007).
13. U. Schnars, T. M. Kreis, and W. P. O. Jüptner, "Digital recording and numerical reconstruction of holograms: reduction of the spatial frequency spectrum," *Opt. Eng.* **35**(4), 977–982 (1996).
14. N. Demoli, H. Halaq, K. Sariri, M. Torzynski, and D. Vukicevic, "Undersampled digital holography," *Opt. Expr.* **17**(18), 15842–15852 (2009).
15. T. Kreis and W. Jüptner, "The suppression of the dc term in digital holography," *Opt. Eng.* **36**, 2357–2360 (1997).
16. T. Kreis, P. Aswendt, and R. Höfling, "Hologram reconstruction using a digital micromirror-device (DMD)," *Opt. Eng.* **40** (2001).
17. I. Yamaguchi and T. Zhang, "Phase-shifting digital holography," *Opt. Lett.* **22**(16), 1268–1270 (1997).
18. M. Takeda, H. Ina, and S. Kobayashi, "Fourier-transform method of fringe-pattern analysis for computer-based topography and interferometry," *J. Opt. Soc. Am.* **72**(1), 156–160 (1982).
19. T. Meeser, C. v. Kopylow, and C. Falldorf, "Advanced digital lensless Fourier holography by means of a spatial light modulator," *IEEE Proc. 3DTV-Con 04 The True Vision-Capture, Transmission and Display of 3D Video* (2010).
20. S. De Nicola, P. Ferraro, A. Finizio, and G. Pierattini, "Correct-image reconstruction in the presence of severe anamorphism by means of digital holography," *Opt. Lett.* **26**(13), 974–976 (2001).
21. S. De Nicola, P. Ferraro, A. Finizio, and G. Pierattini, "Compensation of aberrations in Fresnel off-axis digital holography," *Proc. Fringe 2001*, pp. 407–412 (2001).

Jan Mundt studied physics in Bremen from 2003 to 2009. He passed his diploma thesis at the Bremer Institut für Angewandte Strahltechnik (BIAS). The main task in this thesis was the investigation of lens arrangements in digital holography. The aim was to minimize the angle of the wave fields for holographic recording of large objects. In April 2009 he joined the Department of Modelling and Materials at BIAS. The main issue of his work is to determine heat treatment processes to minimize distortion. His project is involved in the Collaborative Research Centre SFB 570 "Distortion Engineering," which is funded by the German Research Foundation.

Thomas Kreis received his diploma in mathematics from the University of Göttingen. He spent three years as a research assistant at the Institute for Metrology in Engineering, University of Hannover, where he obtained his PhD in mechanical engineering. He joined the Bremer Institut für Angewandte Strahltechnik (the Bremen Institute for Applied Beam Technology) in 1980, where he was first responsible for the field of fundamentals and data processing. Since 1986 he headed the Department of Laser Metrology at BIAS. He received the habilitation in applied optics from the University of Bremen. His research activities range from mathematical methods in optics and laser applications to image processing and coherent optical metrology. His main interest is in computer-aided holographic interferometry. He is the 1987 recipient of the Hans-Rottenkolber Award for outstanding contributions in laser-assisted metrology. He is a member of SPIE, OSA, and DGaO.